16TH EUROPEAN CONFERENCE ON EARTHQUAKE ENGINEERING THESSALONIKI 18 - 21 JUNE 2018

SEISMIC BEHAVIOUR OF CUBE OF ZOROASTER TOWER USING THE DISTINCT ELEMENT METHOD

Amin MOHEBKHAH[1], Vasilis SARHOSIS[2], Elham TAVAFI[3]

ABSTRACT

There are several ancient stone masonry structures of great archeological significance in earthquake prone areas around the world. Ka'ba-ye Zartošt (Cube of Zoroaster) is a 14.2 m square in shape tower, which was built using white limestone blocks and dry joints. The tower dates back to the Achaemenid empire era and is located in the earthquake prone area of Pasargadae in Iran. Although, after approximately 2,500 years the tower is still standing, it is now in a severely deteriorated condition and may be vulnerable against future large in magnitude earthquakes. This paper aims to present the development of a three dimensional numerical model based on the discrete element method of analysis which was used to investigate the seismic behavior of the Cube of Zoroaster tower. To this end, the behavior of the tower to different ground shaking motions is discussed and the possible failure modes for each case are explored.

Keywords: Stone masonry; Ancient monument; Distinct Element Method; Seismic behavior; Ka'ba-ye Zartošt

1. INTRODUCTION

There are many ancient monuments (e.g. multi-drum columns, colonnades and towers) of great architectural and archeological significance around the world. Most of these have experienced major earthquakes during their life. Although some of them that still standing, there are examples where collapses occurred in the past (e.g. the 2,500 years old citadel of the city of Bam, the frescoed vault of the Basilica of St. Francis of Assisi in Perugia, Italy etc.). For engineers, it is important to first understand the behavior of historic masonry structures when subjected to strong ground excitations in order to propose options for repair and strengthening.

A large majority of historic masonry structures have been constructed with dry joints. According to Psycharis et al. (2011), during strong earthquakes, their behavior is characterized by high non-linearity which is governed by sliding, rocking, wobbling and/or complete detachment of adjacent masonry blocks. Thus, failure is usually at the block-to-block joint interface rather than in the blocks (e.g. cracking or crushing of the masonry units).

Today, there are several approaches to model the mechanical behavior of masonry structures (Sarhosis et al. 2016). Housner (1963) was the first to investigate analytically the behavior of rigid single degree of freedom blocks subjected to horizontal excitations. With formulations derived, it is possible to estimate the minimum horizontal acceleration at the base to cause overturning of the rigid body. However, for closely packed multi degree of freedom blocks such as stone masonry towers, analytical solutions are not available. However, with advances in computer power, numerical procedures could be used to obtain the dynamic performance of historic masonry structures subjected to strong seismic excitations.

Research undertaken in the past (Bui et al. 2017; Azevedo et al. 2000; Psycharis et al. 2003) demonstrate

[1]Assistant Prof., Dept. of Civil Engineering, Malayer University, Malayer, Iran, amoheb@malaueru.ac.ir
[2]Assistant Prof., School of Engineering, Newcastle University, Newcastle upon Tyne NE1 7RU, UK, Vasilis.Sarhosis@newcastle.ac.uk
[3]Masters Student, Dept. of Civil Engineering, Malayer University, Malayer, Iran, etavafi@yahoo.com

that the discrete/distinct element method (DEM) can be effectively used to simulate the in-plane and out-of-plane nonlinear behavior of masonry structures constructed with dry joints. Discrete/distinct element method developed by Cundall (1971) to investigate the behavior of jointed rocks where continuity between the separate blocks of rock did not exist. This has similarities with low bond strength masonry or masonry constructed with dry joints where failure is occurring at the joint rather than the masonry unit itself. In addition, within DEM, large displacements, rotations and complete detachments between the blocks is allowed (Itasca 2004). The approach has been used with success to study blocky dry joint masonry structures and monuments subjected to static and dynamic loads (Azevedo et al. 2000, Psycharis et al. 2000, 2003, 2013, Papantonopoulos et al. 2002, Komodromos et al. 2008, Papaloizou and Komodromos 2009, 2012, DeJong et al. 2012, Sarhosis et al. 2015, Sarhosis et al. 2016 a,b, Çakti et al. 2016, Pulatsu et al. 2017). For example, Psycharis et al. (2000), Papantolopoulos et al. (2002, Psycharis et al. (2013) successfully investigated the seismic behavior of freestanding multi-drum columns. It was found that multi-drum columns are more vulnerable to long-period ground motions than short-period ones.

DeJong and Vibert (2012) made use of the three-dimensional software 3DEC based on the DEM to investigate the seismic response of a damaged stone masonry spire in UK. Later, Çakti et al. (2016) used DEM to simulate the seismic behavior of a scaled stone masonry mosque with dry joints tested in a shaking table. Numerical results in good agreement with those obtained from the experiment. They observed that for lower levels of the input motion, the frequency characteristics of the DEM model correlate fairly well with the tested model response characteristics.

Two- and three-dimensional dynamic behavior of the two-story colonnade of the Forum in Pompeii in Italy was investigated by Sarhosis et al. (2016 a & b) using the specialized DEM software UDEC and 3DEC, respectively. They observed that for low-frequency excitations, the failure mode of the colonnade is rocking. While, mode for high-frequency excitations, the failure is a complex combination of sliding and rocking failure modes (2016a). Furthermore, they found that owing to the existence of initial geometric eccentricities, the colonnade structure can vibrate bi-directionally under the in-plane excitations (2016b).

The purpose of this paper is to investigate the 3D nonlinear seismic behavior of the dry joint stone masonry tower of Ka‘ba-ye Zartošt (Cube of Zoroaster) in Persepolis, Iran. A three-dimensional discrete element model has been developed. Use made of the commercial software 3DEC (Itasca, 1998). The intention was to investigate the structural behavior and failure mode of the Cube of Zoroaster tower when subjected to strong earthquake vibrations.

2. DESCRIPTION OF THE MONUMENT

Ka‘ba-ye Zartošt (Cube of Zoroaster), as shown in Fig. 1, is a square tower built of white limestone blocks placed on top of each other. The tower was built during the pre-Persepolitan phase of the Achaemenid monumental architecture (*ca.* 559-511 B.C.) (Schmidt 1970) in Pasargadae, Iran. The tower has been constructed in two levels. The lower level has no voids. Stone unit were placed in regular interval and contain the entire space of the lower level of the tower. The upper part of the tower contains a thick stone wall around the perimeter of the tower as well as some false/blind windows of dark gray limestone and an entrance in the north side. The slightly pyramidal roof of the tower was made of stone blocks tied together using metal clamps. However, there is no steel clamp in its current state. The foundation of the Tower is an approximately square terraced pyramid of three steps made of large stone slabs (Schmidt 1970). Although the foundation slabs have different thicknesses, they have been laid in level surface.

Prior to the archeological excavations of Prof. Schmidt from the Oriental Institute, University of Chicago in June 1939, the lower part of the Tower was buried beneath debris (Schmidt 1970). The staircase which gave access to the main room of the Tower, was built of stone blocks. However, the exposed blocks of the upper part of the staircase have been demolished. Today, only eight steps are preserved. The portion of the north wall behind the upper part of the staircase has been mostly destroyed. The Cube of Zoroaster tower is square in plan with dimensions of 7.30 m on each side (Schmidt 1970). However, there are four ornamental piers in its corners of approximately 1.30 m on each side. The total maximum height of the Cube of Zoroaster tower including the steps of the base is 14.12 m. The average height of

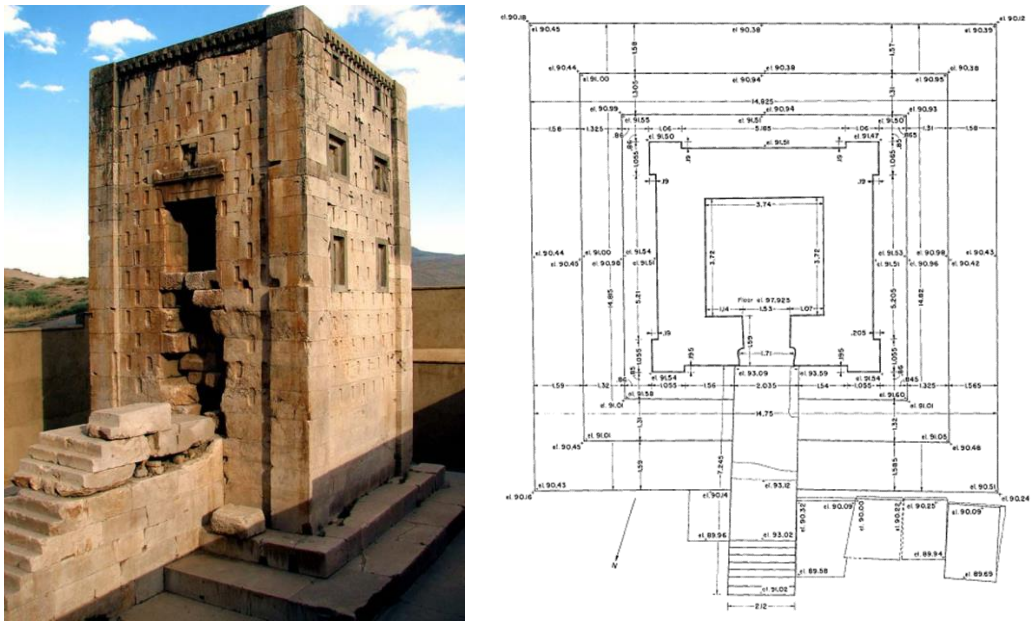

Figure 1. (a) Northwest view, and (b) plan of the Achaemenid tower (Schmidt 1970)

the stone courses is 0.5 m. The upper level of the tower is almost square with dimensions (3.72m × 3.74 m). The walls' thickness ranges from 1.54 to 1.62 m. The height of the tower room is 5.54 m.

3. DISCRETE ELEMENT METHOD

3DEC is an advanced numerical modelling code based on DEM for discontinuous modelling and can simulate the response of discontinuous media, such as masonry, subjected to either static or dynamic loading. When used to model masonry, the units (i.e. stones) are represented as an assemblage of rigid or deformable blocks which may take any arbitrary geometry. Typically, rigid blocks are adequate for structures with stiff, strong units, in which deformational behaviour takes place at the joints. For explicit dynamic analysis, rigid block models run significantly faster. For static problems, this computational advantage is less important, so deformable blocks are preferable, as they provide a more elaborate representation of structural behaviour. Rigid blocks, were used in the analyses reported herein. Joints are represented as interfaces between blocks. These interfaces can be viewed as interactions between the blocks and are governed by appropriate stress-displacement constitutive laws. These interactions can be linear (e.g. spring stiffness) or non-linear functions. Interaction between blocks is represented by set of point contacts, of either vertex to face or edge to edge type (Fig. 2). In 3DEC, finite displacements and rotations of the discrete bodies are allowed. These include complete detachment between blocks and new contact generation as the calculation proceeds. Contacts can open and close depending on the stresses acting on them from the application of the external load. Contact forces in both the shear and normal direction are considered to be linear functions of the actual penetration in shear and normal directions, respectively (Itasca 2004). In the normal direction, the mechanical behaviour of joints is governed by the following equation:

$$\Delta\sigma_n = - JK_n \cdot \Delta u_n \qquad (1)$$

where JK_n is the normal stiffness of the contact, $\Delta\sigma_n$ is the change in normal stress and Δu_n is the change in normal displacement. Similarly, in the shear direction the mechanical behaviour of mortar joints is controlled by a constant shear stiffness JK_s using the following expression:

$$\Delta\tau_s = - JK_s \cdot \Delta u_s \qquad (2)$$

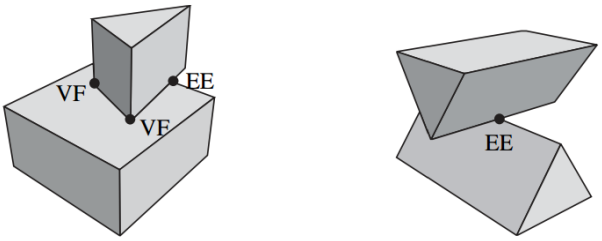

Figure 2. Representation of block interaction by elementary vertex-face (VF) and edge-edge (EE) point contacts in 3DEC (Lemos 2007)

where $\Delta\tau_s$ is the change in shear stress and Δu_s is the change in shear displacement. These stress increments are added to the previous stresses, and then the total normal and shear stresses are updated to meet the selected non-elastic failure criteria, such as the Mohr-Coulomb model.
The calculations are made using the force-displacement law at all contacts and the Newton's second law of motion at all blocks. The force-displacement law is used to find contact forces from known displacements, while the Newton's second law governs the motion of the blocks resulting from the known forces acting on them. Convergence to static solutions is obtained by means of adaptive damping, as in the classical dynamic relaxation methods.

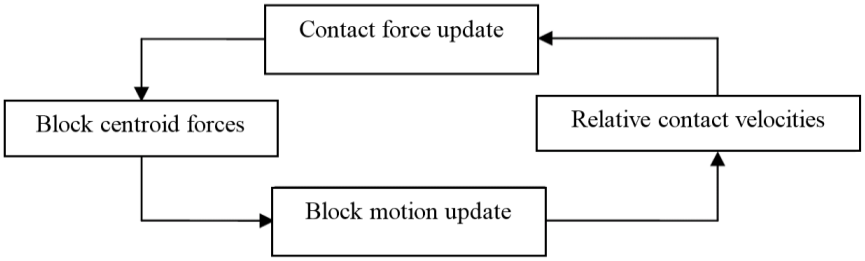

Figure 3 shows the schematic representations of the calculations taking place in 3DEC analysis.

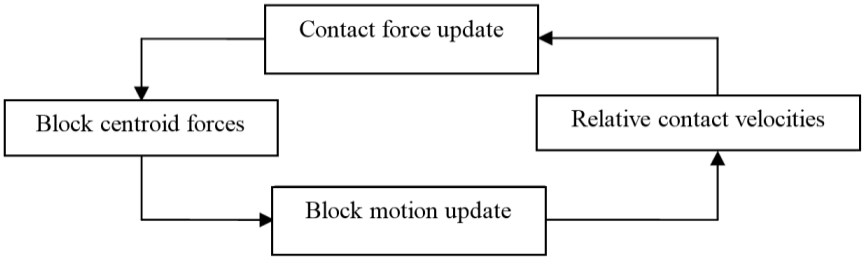

Figure 3. Calculation cycle in 3DEC (Itasca 2004)

4. DEM MODELING OF THE TOWER

4.1 Geometry and material properties

A geometric model to represent the current condition of the tower has been developed as shown in Fig. 4. Blocks assumed to behave as rigid elements connected together by a zero thickness interface. Thus, the nonlinear behavior of the structure is at the block-to-block interface.
The unit weight of the limestone masonry blocks was considered to be 2680 kg/m^3. The joints' normal and shear stiffness parameters (i.e., JK_n and JK_s) can be evaluated from the stiffness of the real joint under the assumption of stack bond (Lourenço et al. 2005). However, due to the lack of experimental data, typical values of 4×10^6 and 2×10^6 kPa/m for the joints' stiffness in the normal and shear directions respectively have been used (Sarhosis et al. 2016b).

The zero thickness interfaces between adjacent blocks were modelled using the Mohr-Coulomb slip model. The angle of internal friction at the block-to-block interfaces were assumed 30°. Since the tower has been constructed with dry joints, both the cohesion and tensile strength at the interfaces were zero.

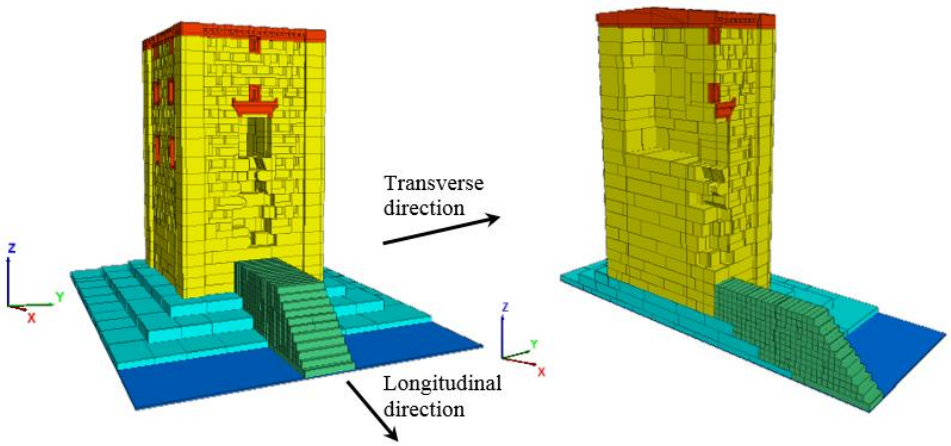

Figure 4. The geometric model developed to represent the actual condition of the tower

4.3 Seismic Input and damping

Initially, gravitation load has been assigned into the system. Then, the system brought into equilibrium under its own weight where the unbalance forces checked whether they are constant and almost equal to zero. Ground motion obtained from the Tabas earthquake were applied at the base of the tower, in both the longitudinal direction (i.e. along the direction where the staircase is located, x-axis, see Figure 4) and transverse direction (i.e. perpendicular to the staircase, y-axis, see Figure 4). The Tabas earthquake occurred on the 16th of September 1978 in central Iran. The earthquake had 7.3 Richter magnitude. The PGA of longitudinal and transverse components of the record was 0.85g and 0.86g, respectively. Figure 5 shows the acceleration records applied to the tower in the longitudinal and transverse directions. During the dynamic analysis, no viscous damping was assumed, the only dissipation being due to frictional sliding on the joints. This conservative assumption is often used in simulating stone masonry structures containing dry joints (Papantopoulos et al. 2002).

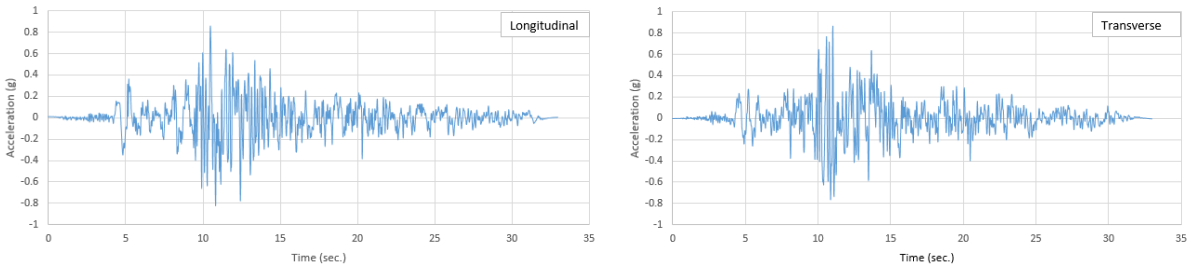

Figure 5. Longitudinal and transverse components of the Tabas acceleration applied to the tower

5. RESULTS AND DISCUSSIONS

The records shown in Figure 5 were applied along: a) the longitudinal direction; b) the transverse direction; and c) both longitudinal and transverse direction of the tower. Also, the time-history of horizontal displacements at the corner points in the roof slab were recoded (i.e. points 1-4 in Figure 6). The results of each analysis are presented and discussed below.

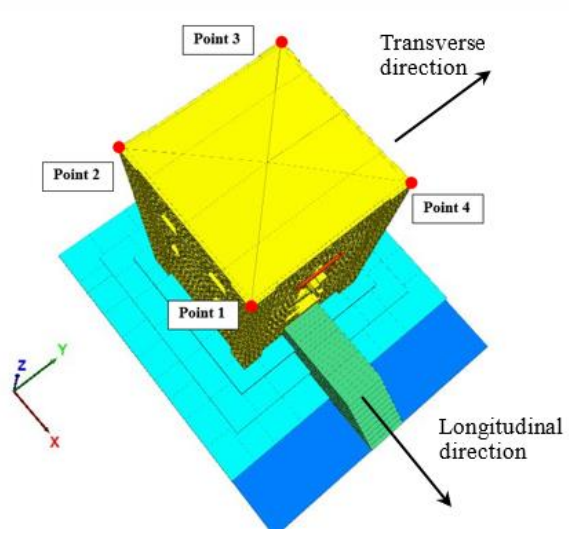

Figure 6. Monitoring points during the dynamic analysis on the roof slab

5.1 Response to the longitudinal excitation

Initially, the tower was subjected to ground excitations in the longitudinal direction (i.e. along the staircase direction, X-axis). Figure 7 shows the horizontal displacements along the X-axis (in-plane direction) of the four monitoring points against the time that the event took place. From Figure 7, for the first 12 seconds of the earthquake excitation, the horizontal displacement of all the monitoring points are the same. From 12 to 18 seconds of the earthquake excitation, the horizontal displacements of the monitoring point 1, 2 and 4 are equal, while the X-axis horizontal displacement for the control point 3 differs. This is probably due to a slippage of the corner block in the out of plane direction. In addition, from Figure 7, just after the 18th second of the excitation, each side of the roof of tower moves independently to each other. This is an indication that complete separation has occurred between the slabs of the roof. Finally, from time equal to 25 second and until the end of the simulation, the roof oscillates around the permanent lateral displacements of ± 0.05 m.

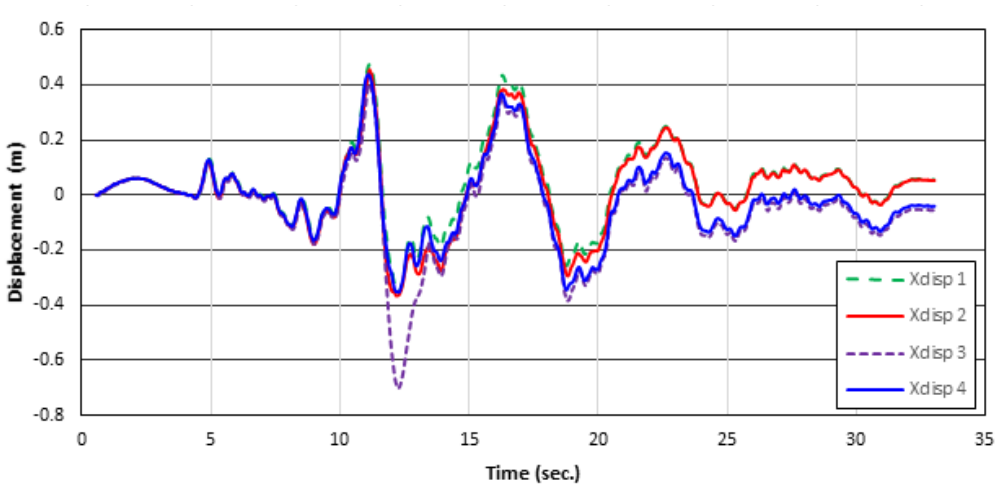

Figure 7. Comparison of the in-plane displacement of the monitored points under the longitudinal excitation

Figure 8 shows the variation of the displacement in the Y-axis (out-of-plane direction) for the four monitoring points when the tower is subjected to longitudinal excitation. From Figure 8, for the first 5 seconds of the earthquake excitation, the roof of the tower does not move. However, just after the first 5 seconds of the excitation, the behavior of the tower is non-linear. In particular after the 17th second of the excitation a complete detachment of the slabs of the roof is observed since both sides edges displace

in opposite directions to each other developing a torsional coupling response. This phenomenon is also shown in the failure mode of the tower, Figure 9. Also, in the in plane to the earthquake load direction, the maximum displacement is 0.43 m while in the out of plane direction is only 0.025 m.
From Figure 9 it is evident that the upper part of the tower undergoes a sliding shear failure mode. This mode is deformation-controlled which makes the structure to sustain large lateral drifts without global instability. This ductile behavior may be attributed to the size effect due to the use of large size pieces of stone blocks in the tower compared to its overall dimensions.

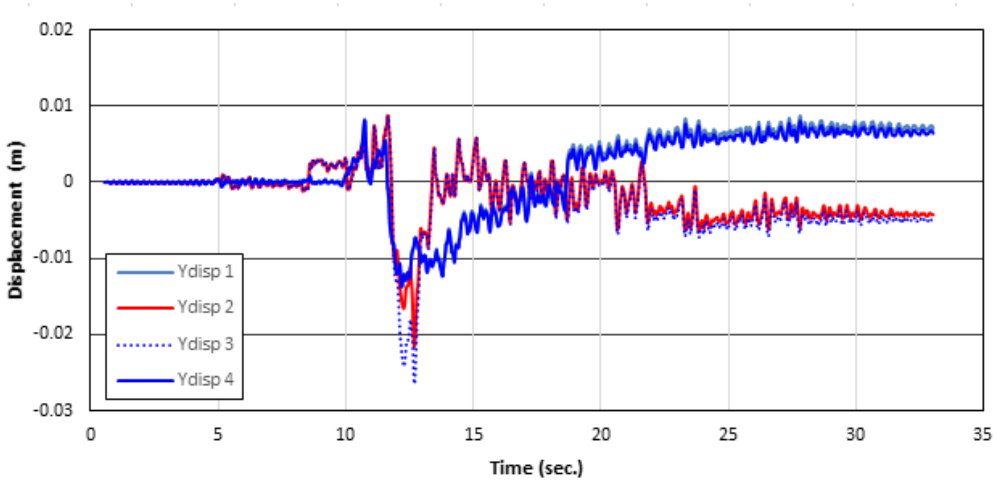

Figure 8. Comparison of the out-of-plane displacement of the monitored points under the longitudinal excitation

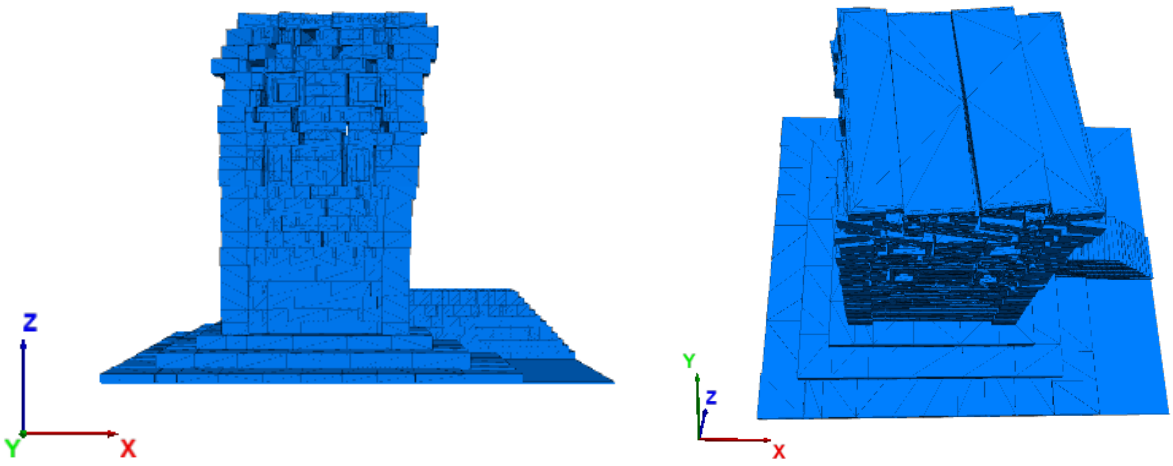

Figure 9. Deformed geometry of the tower under the longitudinal excitation (magnification factor =10), time 33 seconds

5.2 Response to the transverse excitation

The tower was also subjected to horizontal excitations in the transverse direction (i.e. direction perpendicular to the staircase). Figure 10 shows the in-plane horizontal displacement along the X-axis of the four monitored points when the tower was subjected to seismic load in the transverse direction. From Figure 10, for the first 8 seconds of the earthquake excitation, the tower behaves as a solid element. So, all points move approximately the same. However, from the 8th to the 23rd seconds of earthquake excitation, the behavior of the tower is highly nonlinear. In particular, monitoring points 2 and 3 displace in the opposite direction to the monitoring points 1 and 4. The maximum displacement recorded was at

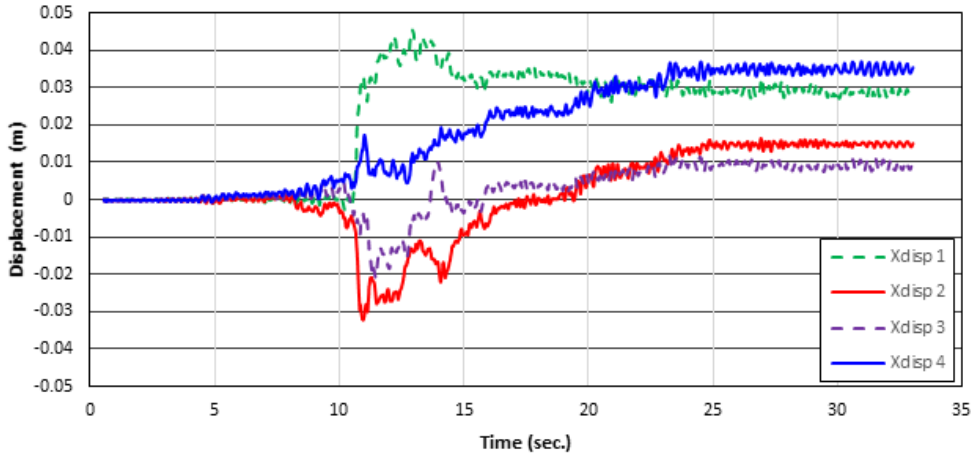

Figure 10. Comparison of the out-of-plane displacement of the monitored points under the transverse excitation

point 1 and found to be equal 45 mm. From the 23rd second and onward, the roof oscillates around the permanent lateral displacements of 30 mm for the control points 1 and 4 and 10 mm for the control points 2 and 3.

Figure 11 shows the in-plane displacement along the Y-axis for the monitored points when the tower is subjected to transverse excitation (direction perpendicular to the staircase). From Figure 11, during the entire earthquake excitation, the horizontal displacements for all the four monitoring points are the same and this is an indication that there is no collapse/detachment of blocks of the roof of the tower. However, it is worth mentioning that the maximum displacement is more than 1 meter which is significantly higher to the maximum displacement of the tower in the out of plane direction (i.e. X-axis direction).

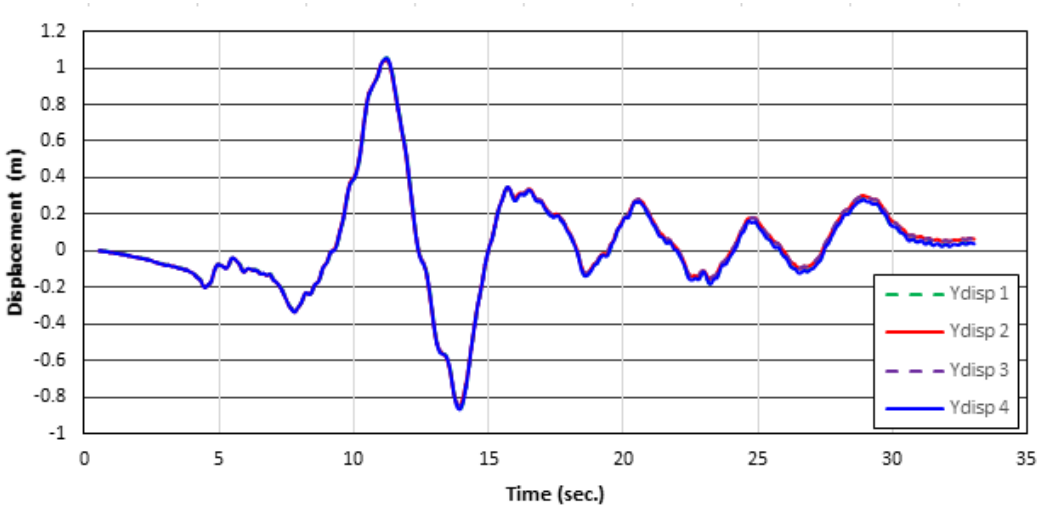

Figure 11. Comparison of the in-plane displacement of the monitored points under the transverse excitation

Figure 12 shows the deformed shape of the structure at the end of the simulation. From Figure 12, the upper half part of the tower undergoes a sliding shear failure towards the right hand side. Such failure mode could be described by a deformation-controlled mechanism, which makes the structure to sustain large lateral drifts without global instability. In addition, vertical cracks appeared from the top to the middle right hand side of the tower. This failure mode is similar to the failure mode observed when the load applied in the longitudinal direction.

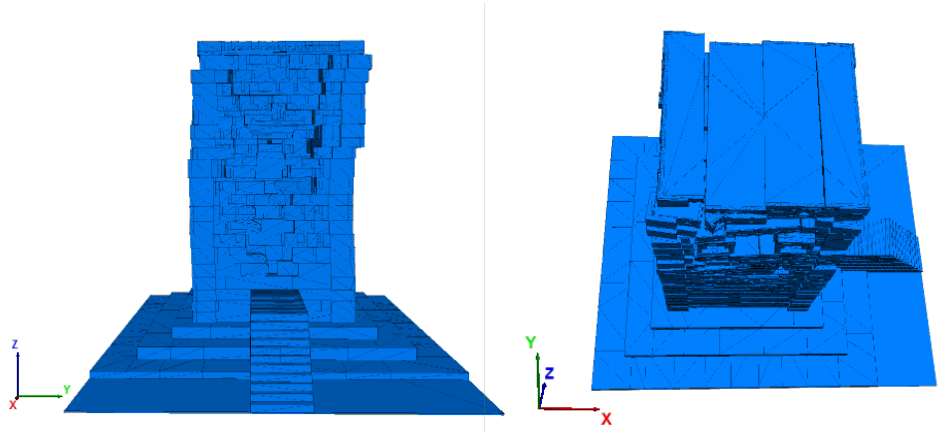

Figure 12. Deformed geometry of the tower under the transverse excitation (magnification factor =10), time 33 seconds

5.3 Response to the bi-directional excitation

The tower subjected to ground excitations in both transverse (i.e. perpendicular to the staircase, Y-axis) and longitudinal direction (i.e. along the staircase direction, X-axis). Figure 13 shows the horizontal displacements along the X-axis for the four monitoring points during the application of the earthquake load. From Figure 13, the horizontal displacement of all the monitoring points have the same pattern. In particular, up to the first 12 second of the earthquake excitation, the roof behaves as a single element and all four monitoring points displace the same. However, from the 12th second and until the end of the simulation, the horizontal displacements at control points is different and the tower is behaving non-linearly. In particular, the horizontal displacement of the control points 1 and 4 is larger to the one of control points 2 and 3. This is an indication that torsional failure mode occurred.
Similarly, Figure 14 shows the variation of the y-axis displacement of the monitored points under the bi-directional excitation. From Figure 14, for the first 15 seconds of the earthquake excitation, the roof of the tower is rigid and behaves as a single element. Thereafter, the control points 1, 2 and 3, 4 are behaving as pairs in a similar manner. In particular, after 15 seconds of the earthquake excitation, the roof oscillates at a maximum value of 0.6 m for the control points 2 and 3 and 0.4 m for the control points 1 and 4. The deformed geometry of the structure is shown in Figure 15. From Figure 15, it is evident that the connection of the top slab of the tower has been lost. In addition, the upper part of the tower undergoes a sliding shear failure.

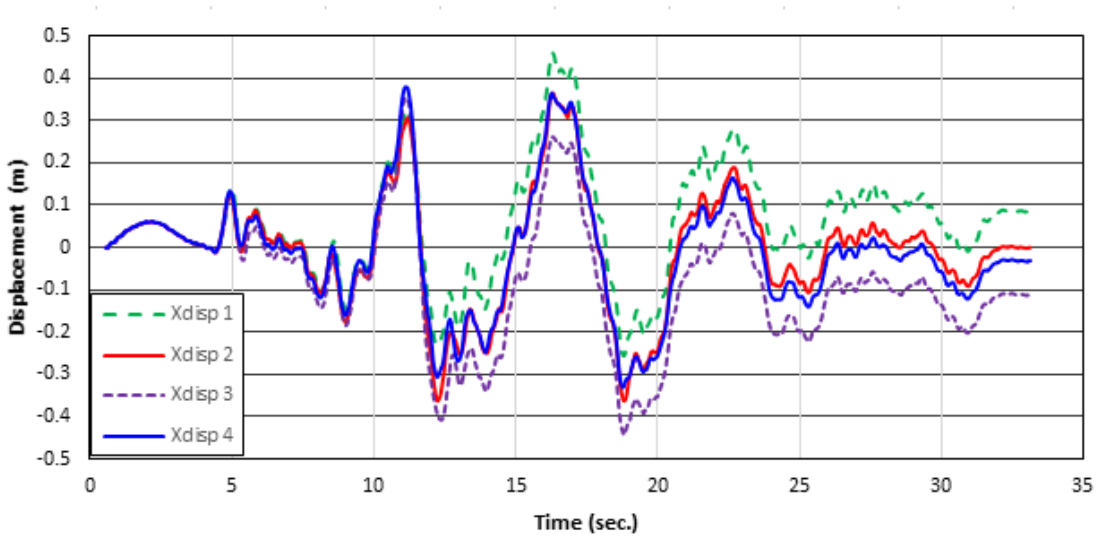

Figure 13. Comparison of the x-direction displacement of the monitored points under the bi-directional excitation

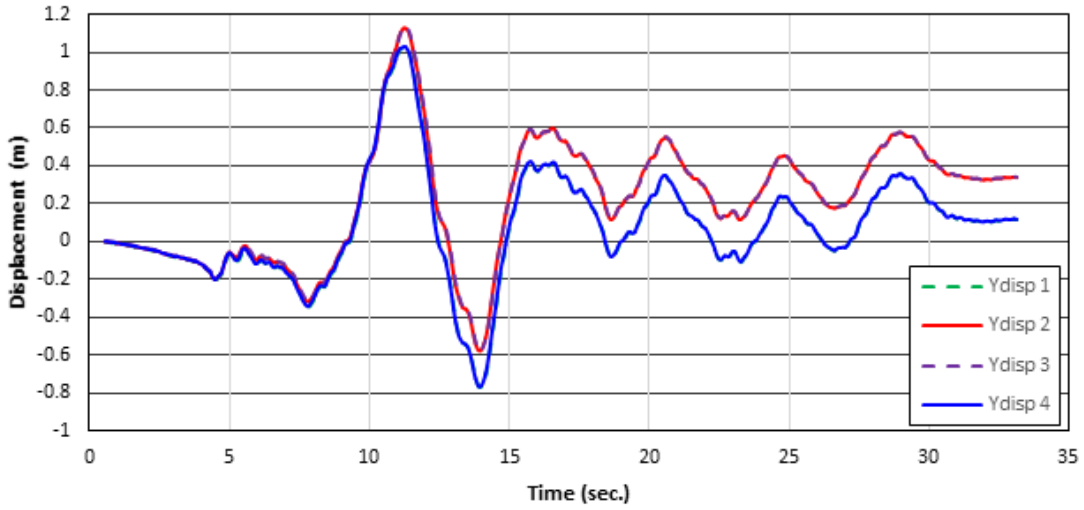

Figure 14. Comparison of the y-direction displacement of the monitored points under the bi-directional excitation

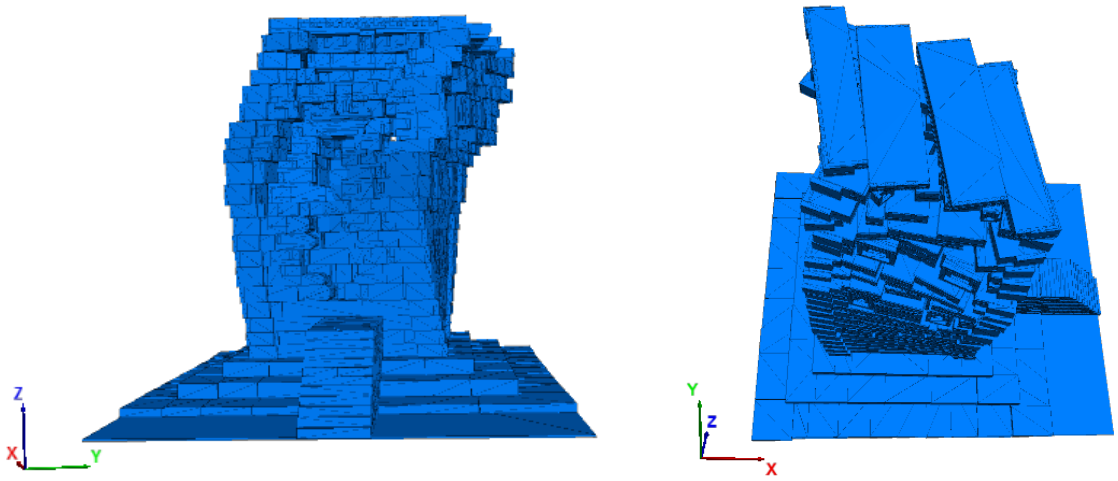

Figure 15. Deformed geometry of the Tower under the bidirectional excitation (magnification factor =10)

5.4 Comparison of the maximum lateral displacements of the control points

Table 1 compares the lateral displacements for the four control points as obtained for all the simulations. From Table 1, when the tower is subjected to excitations in the longitudinal direction, the maximum lateral displacement occurs at control point 3 and it is along the X-axis (in-plane direction). Alternatively, when the tower is subjected to horizontal excitations in the transverse direction, the maximum lateral displacement occurs at control point 1 ad 4 along the Y-axis (in-plane direction). Moreover, when the tower is subjected to excitation in both the transverse and longitudinal direction, the maximum lateral displacement occurs at points 2 and 3 along the Y-axis. Finally, from Table 1, we can observe that the tower suffers largest displacements in the Y-axis direction (i.e. direction perpendicular to the staircase). Comparing the three cases together, we can conclude that the largest horizontal displacement occurs when the excitation is applied in bi-lateral direction for the control points 2 and 3 and is equal to 1.12 m in the Y-axis direction.

Table 1. Maximum lateral displacements of the control points (m).

Control points	Longitudinal direction		Transverse direction		Bi-lateral direction	
	X-disp	Y-disp	X-disp	Y-disp	X-disp	Y-disp
1	0.470	-0.014	0.044	1.030	0.450	1.020
2	0.455	-0.021	-0.032	1.015	0.360	1.120
3	-0.700	-0.026	-0.020	1.015	-0.410	1.120
4	0.435	-0.014	0.035	1.030	0.370	1.020

5. CONCLUSIONS

Using a three dimensional software based on the discrete element method of analysis, an investigation into the seismic behavior of the Ka'ba-ye Zartošt (Cube of Zoroaster) tower located in Persepolis, Iran undertaken. Within the model, the actual geometry of the tower has been generated. Each block of the tower simulated by a rigid element connected together by zero thickness interfaces. Ground motions obtained from the Tabas earthquake were used and applied at the base of the tower in the longitudinal direction; the transverse direction; and in both longitudinal and transverse direction. The PGA of longitudinal and transverse components of the record was 0.9g and 0.8g, respectively. Also, the time-history of horizontal displacements at the corner points in the roof slab of the tower were recoded. From the results analysis, it can be observed that the seismic behavior of the tower is highly influenced by the magnitude and direction of load applied on it. When the tower subjected to earthquake excitations in one direction, the maximum lateral displacement of the control points was higher at the direction where the earthquake excitation applied. Thus, the tower is strong in the out of plane direction. The tower is more vulnerable when earthquake excitations are applied in the transvers direction rather than the longitudinal one. When the tower subjected to excitations in the longitudinal direction, the maximum lateral displacement found to be 0.7 m and occurred at control point 3 along the X-axis (in-plane direction). However, when the tower subjected to horizontal excitation in the transverse direction, the maximum lateral displacement found to be 1.03 m and occurred at control point 1 and 4 along the Y-axis (in-plane direction). For all cases studied, it was found that the tower is most vulnerable when it is subjected to horizontal excitations in both the transverse and longitudinal direction. The maximum lateral displacement found to be 1.12 m and occurred at points 2 and 3 along the Y-axis (i.e. direction perpendicular to the staircase). The failure mode of the tower was a combination of both shear and torsional failure. Such failure mode allowed the structure to sustain large lateral drifts without global instability. This ductile behavior could be due to the relatively large size of the stone blocks compared to the size of the tower.

6. ACKNOWLEDGMENTS

The authors are grateful to Professor I.N. Psycharis for his useful comments regarding this research numerical simulations.

7. REFERENCES

Azevedo JJ, Sincraian GE, Lemos JV (2000). Seismic behavior of blocky masonry structures. *Earthquake Spectra*, 16(2): 337–365.

Bui TT, Limam A, Sarhosis V, Hjiaj M. (2017). Discrete element modelling of the in-plane and out-of-plane behaviour of dry-joint masonry wall constructions. *Engineering Structures*, 136: 277-294.

Çakti E, Saygili Ö, Lemos JV, Oliveira CS (2016). Discrete element modeling of a scaled masonry structure and its validation. *Engineering Structures*, 126: 224-236.

Cundall PA (1971). A computer model for simulating progressive large scale movements in blocky rock systems. *Proceedings of the 2nd Symposium of the International Society of Rock Mechanics, Vol. 1, Paper No II-8, Nancy, France.*

DeJong MJ, Vibert C (2012). Seismic response of stone masonry spires: computational and experimental modeling. *Engineering Structures*, 40: 566-574

Housner, G. W. (1963). The behavior of inverted pendulum structures during earthquakes. Bulletin of Seismological Society of America, 53(1), 403–17.

Itasca (2004). 3DEC: 3-Dimensional Distinct Element Code. Theory and Background, *Itasca consulting group*, Minneapolis, USA.

Komodromos P, Papaloizou L, Polycarpou P (2008). Simulation of the response of ancient columns under harmonic and earthquake excitations. *Engineering Structures*, 30(8): 2154-2164.

Lourenço PB, Oliveira DV, Roca P, Orduna A (2005). Dry joint masonry walls subjected to in-plane combined loading, *Journal of Structural Engineering*, 131(11): 1665-1673.

Psycharis IN, Papastamatiou DY, Alexandris AP (2000). Parametric investigation of the stability of classical columnsunder harmonic and earthquake excitations. *Earthquake Engineering and Structural Dynamics*, 29(8): 1093-1109.

Psycharis IN, Lemos JV, Papastamatiou DY, Zambas C, Papantonopoulos C (2003). Numerical study of the seismic behaviour of a part of the Parthenon Pronaos. *Earthquake Engineering and Structural Dynamics*, 32(13): 2063-2084.

Psycharis IN, Drougas AE, Dasiou M-E AM (2011). Seismic behaviour of the walls of the Parthenon: a numerical study. In: Papadrakakis M, Fragiadakis M, Lagaros ND (eds): Computational Methods in Earthquake Engineering, *Computational Methods in Applied Sciences* 21, , Springer Netherlands, pp 265-283.

Psycharis IN, Fragiadakis M, Stefanou I (2013). Seismic reliability assessment of classical columns subjected to near-fault ground motions. *Earthquake Engineering and Structural Dynamics*, 42(14): 2061-2079.

Papantonopoulos C, Psycharis IN, Papastamatiou DY, Lemos JV, Mouzakis HP (2002). Numerical prediction of the earthquake response of classical columns using the distinct element method. *Earthquake Engineering and Structural Dynamics*, 31(9): 1699-1717.

Papaloizou L, Komodromos P (2009). Planar investigation of the seismic response of ancient columns and colonnades with epistyles using a custom-made software. *Soil Dynamics and Earthquake Engineering*, 29(11-12): 1437-1454.

Pulatso B, Sarhosis V, Bretas E, Nikitas Nikolaos, Lourenço PB. (2017). Non-linear static behaviour of ancient free-standing stone columns. *Proceedings of the Institute of Civil Engineers- Structures and Buildings*, 170(6): 406-418.

Sarhosis V. (2016). Micro-modelling options for masonry structures. In: Sarhosis V., Lemos J.V., Bagi K., Milani G, ed. Computational Modelling of Masonry Structures Using the Discrete Element Method. IGI Global.

Sarhosis V, Lignola GP, Asteris PG (2015). Seismic Vulnerability of Ancient Colonnade: Two storey colonnade of the Forum in Pompeii. In: Plevris V, Asteris P. (eds), Seismic Assessment and Rehabilitation of Historic Structures, *IGI Global*, pp 331-358.

Sarhosis V, Asteris P, Wang T, Hu W, Han Y (2016 a). On the stability of colonnade structural systems under static and dynamic loading conditions. *Bull. Earthquake Eng.*, 14(4): 1131-1152.

Sarhosis V, Asteris PG, Mohebkhah A, Xiao J, Wang T. (2016 b). Three dimensional modelling of ancient colonnade structural systems subjected to harmonic and seismic loading. *Structural Engineering and Mechanics*, 60(4), 633-653.

Schmidt EF (1970). Persepolis III: The Royal Tombs and other Monuments, The oriental Institute Publications, Volume LXX, The University of Chicago, Chicago, Illinois, USA.